A model for fire-induced sediment yield by dry ravel in steep landscapes

Michael P. Lamb,[1] Joel S. Scheingross,[1] William H. Amidon,[1] Erika Swanson,[1] and Ajay Limaye[1]

Received 8 September 2010; revised 19 April 2011; accepted 28 April 2011; published 29 July 2011.

[1] Sediment flux from hillslopes to channels commonly increases following wildfires, with implications for the carbon cycle, river habitats, and debris-flow hazards. Although much of this material is transported via dry ravel, existing ravel models are not applicable to hillslopes with gradients greater than the angle of repose, which can constitute the majority of mountainous terrain. To fill this knowledge gap, we develop a continuity model for sediment storage by vegetation dams on steep hillslopes to predict sediment yields following wildfire. The maximum volume of sediment stored prior to wildfire is set to be a function of vegetation density, the capacity of plants to impound sediment, and the contributing hillslope area. Time is required after fire to establish vegetation and replenish hillslope sediment storage, which introduces vegetation regrowth rate, soil production rate, and fire recurrence interval as important variables that affect ravel yield. Model results for the San Gabriel Mountains, California, predict that sediment yield can increase by several orders of magnitude following fire. These results are consistent with field data of ravel yield (~30 mm per contributing area of hillslope in 5 months) we collected following the 2009 Station Fire, as well as postfire sediment flux recorded by 93 debris basins. In contrast to previous work, our model shows that heightened postfire sediment yields can be explained by a change in hillslope sediment storage independent of major changes in the soil production rate and landscape form over geomorphic timescales.

Citation: Lamb, M. P., J. S. Scheingross, W. H. Amidon, E. Swanson, and A. Limaye (2011), A model for fire-induced sediment yield by dry ravel in steep landscapes, *J. Geophys. Res.*, *116*, F03006, doi:10.1029/2010JF001878.

1. Introduction

[2] Sediment flux from hillslopes to channels often increases by more than an order of magnitude following fires [*Eaton*, 1935; *Swanson*, 1981; *Wells*, 1981; *Rice*, 1982; *Moody and Martin*, 2001; *Shakesby and Doerr*, 2006; *Jackson and Roering*, 2009]. This can lead to enhanced carbon flux to ocean basins [e.g., *Hunsinger et al.*, 2008], channel infilling that affects fluvial habitats and organisms [*Florsheim et al.*, 1991; *Gamradt and Kats*, 1997; *Reneau et al.*, 2007; *Coffman et al.*, 2010; *Eaton et al.*, 2010] and debris flows that cause loss of life and property [*Eaton*, 1935; *Rice*, 1982; *Wells*, 1987; *Wohl and Pearthree*, 1991; *Spittler*, 1995; *Cannon*, 2001; *Gartner et al.*, 2008; *Jordan and Covert*, 2009; *Cannon et al.*, 2010]. Moreover, because fires can lead to significant changes in sediment flux rates, they may need to be accounted for in landscape evolution models used to predict landform response to climate and tectonics [*Benda and Dunne*, 1997; *Gabet and Dunne*, 2003; *Lavé and Burbank*, 2004; *Roering and Gerber*, 2005].

[3] The dominant processes that deliver sediment from hillslopes to channels following fires are not well understood mechanistically and predictions rely on statistical correlations between sediment yield, basin area, hillslope angle, burn intensity, and other parameters [e.g., *Los Angeles County Flood Control District* (*L.A.C.F.C.D.*), 1959; *Gartner et al.*, 2008; *Cannon et al.*, 2010]. These predictions, while necessary and useful, have large uncertainties. More accurate predictions likely require identification and modeling of dominant erosion processes, explicitly accounting for the physics of sediment production, transport, and storage.

[4] Several processes have received study following fire including dry ravel, shallow landsliding, Horton overland flow, rilling, and wind erosion [e.g., *Shakesby and Doerr*, 2006]. Of these, dry ravel is the dominant sediment delivery mechanism in many steep landscapes following fire [*Krammes*, 1965; *Rice*, 1982; *Florsheim et al.*, 1991; *Gabet*, 2003; *Lavé and Burbank*, 2004; *Roering and Gerber*, 2005; *Shakesby and Doerr*, 2006; *Jackson and Roering*, 2009]. Dry ravel is the process of rolling, bouncing, and sliding of loose material, which often forms depositional cones where

[1]Division of Geological and Planetary Sciences, California Institute of Technology, Pasadena, California, USA.

Copyright 2011 by the American Geophysical Union.
0148-0227/11/2010JF001878

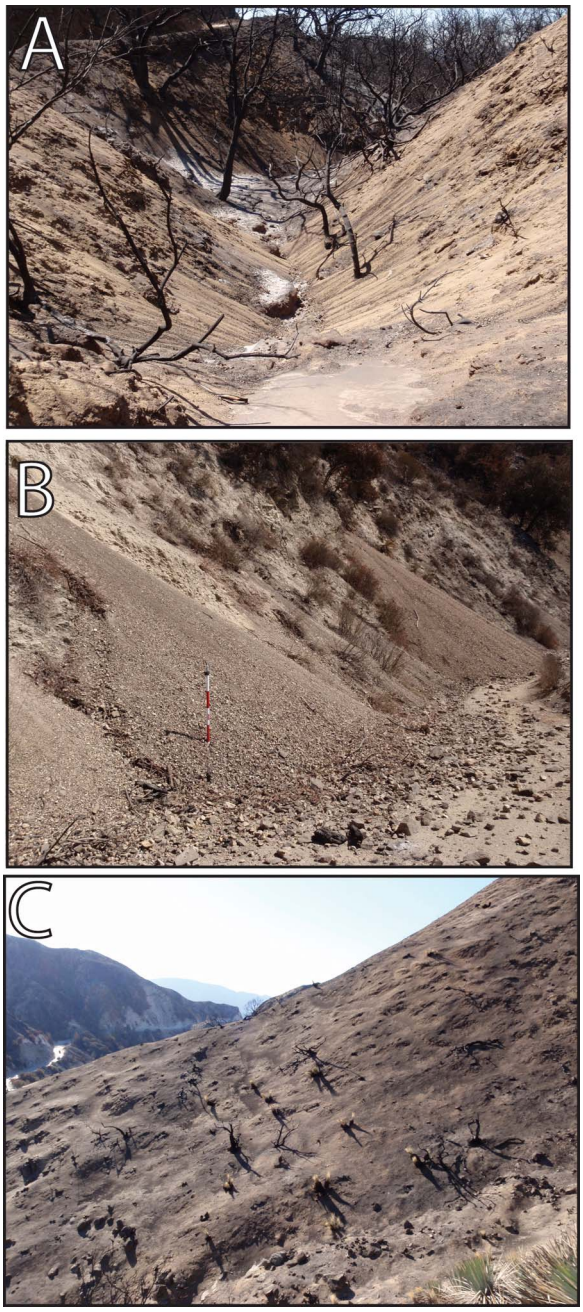

Figure 1. Photographs following the 2009 Station Fire, San Gabriel Mountains, California. Loose silt, sand, and gravel accumulated as ravel cones (a) along the banks of a channel and (b) along a U.S. Forest Service road. Note 1.25 m tall measuring stick with 0.21 m alternating red and white markings for scale. (c) Hillslope showing burned chaparral and yucca plants with mounds of soil upslope that cause a hummocky topography at the scale of several meters. The hillslope gradient was less than the angle of repose so that the landscape maintained a soil mantle postfire.

it reaches slopes less than the angle of repose (Figures 1a and 1b). Most of this material is transported down hillslopes during or immediately following a fire [*Bennett*, 1982; *Florsheim et al.*, 1991; *Jackson and Roering*, 2009].

[5] Quantitative models for dry ravel to date have been formulated for slopes less than the angle of repose (or the internal friction angle of sediment). *Roering and Gerber* [2005] fit a nonlinear flux law to ravel accumulation data to argue that the transport coefficient increased and the critical slope decreased after a fire, resulting in a heightened sediment flux and a heightened long-term erosion rate. *Gabet* [2003] derived a similar expression by considering explicitly the momentum of particles moving down an inclined plane [see also *Furbish et al.*, 2008]. Both models predict that sediment flux is infinite at slopes greater than the angle of repose. On such steep slopes, sediment flux must be limited by sediment supply.

[6] Our inability to model sediment flux following fires on slopes greater than the angle of repose is a significant knowledge gap. In many mountainous landscapes prone to fires, more than 50% of the terrain can have hillslope gradients that exceed 30° (e.g., Oregon Coast Range [*Jackson and Roering*, 2009], San Gabriel Mountains, California [*Rice*, 1982; *DiBiase et al.*, 2010]). Moreover, the greatest ravel fluxes are observed at bases of hillslopes that are steeper than ~30°, with an abrupt increase occurring at about that angle [*Anderson et al.*, 1959; *Krammes*, 1965; *Mersereau and Dyrness*, 1972].

[7] In this paper we first present new measurements of ravel yield following the 2009 Station Fire in the San Gabriel Mountains and an analysis of historic debris basin data in similar catchments. Second, we present a mass balance model to predict ravel flux following fires due to the evacuation of sediment stored behind vegetation on hillslopes with gradients steeper than the angle of repose. We explore the model for an example case, the San Gabriel Mountains, California, where the association between enhanced sediment yield and fire has been well documented [e.g., *Anderson et al.*, 1959; *Krammes*, 1965; *Lavé and Burbank*, 2004]. Finally, we discuss implications for predicting postwildfire sediment flux, debris flow hazards, landscape evolution, and motivation for future work.

2. Ravel Yield Observations

[8] The new model for ravel yield introduced in section 3 was motivated from field observations of postfire ravel yield. These show that ravel yield increases abruptly for hillslopes with average gradients that exceed the angle of repose [e.g., *Anderson et al.*, 1959; *Krammes*, 1965; *Mersereau and Dyrness*, 1972]. Furthermore, the yield increases immediately following a fire and can exceed background, nonfire ravel yields by more than an order of magnitude [e.g., *Bennett*, 1982; *Florsheim et al.*, 1991; *Jackson and Roering*, 2009]. In this section, we briefly review the evidence for these findings including new data of ravel yield we measured following the 2009 Station Fire in the San Gabriel Mountains, California, and an analysis of historic debris basin data from the same area.

[9] We focus on the southern front of the San Gabriel Mountains, California (Figure 2) because wildfires and associated heightened sediment fluxes are common and well documented [e.g., *Anderson et al.*, 1959; *Krammes*, 1965; *Lavé and Burbank*, 2004]. The San Gabriel Mountains are a tectonically active range resulting from a restraining bend in the San Andreas Fault System. The landscape is steep: 60%

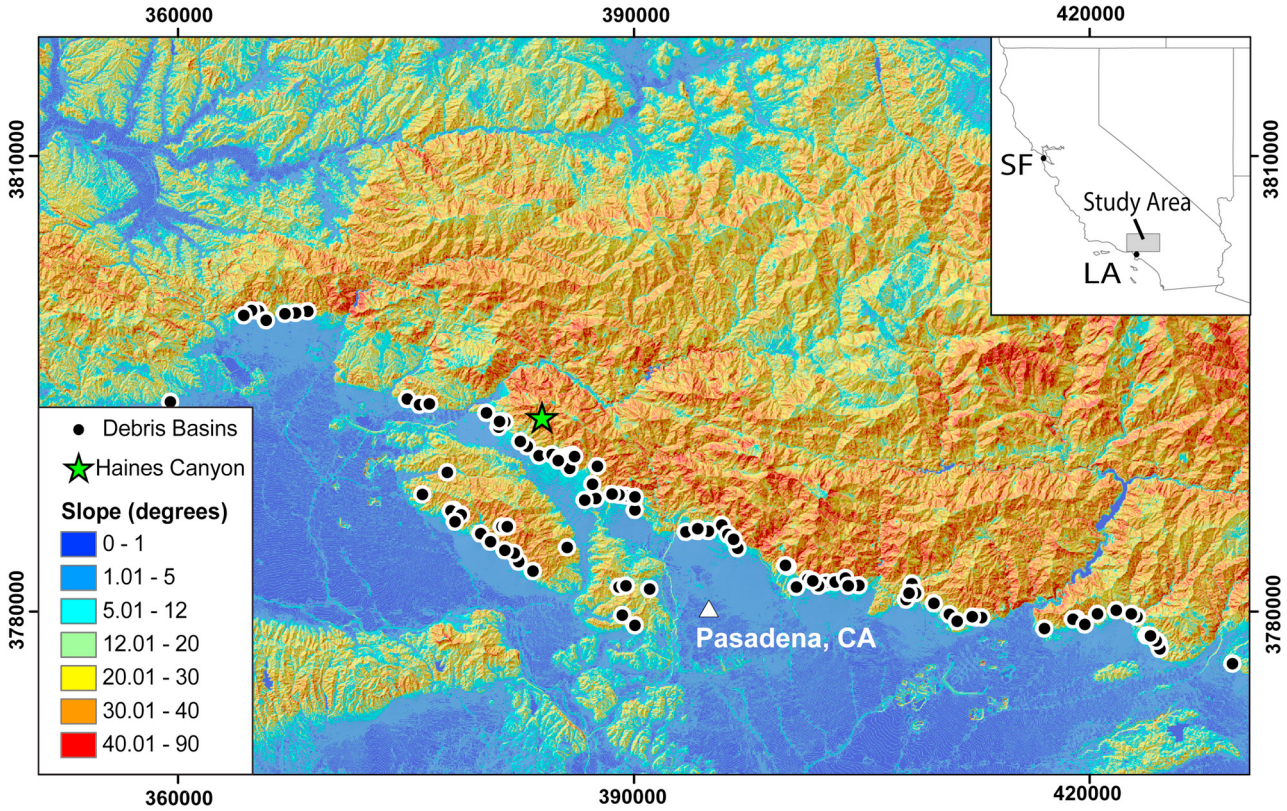

Figure 2. Shaded relief and hillslope map of the San Gabriel Mountains, California, showing locations of Haines Canyon and the debris basins analyzed in sections 6 and 7, respectively. Slope values were generated from the 10 m National Elevation Data Set (U.S. Geological Survey) based on the steepest local slope of each pixel. Note that a significant portion of the landscape is greater than 30° at 10 m scale. Inset map shows an outline of California, the study area, Los Angeles (LA), and San Francisco (SF). Bounding box gives coordinates in UTM.

and 78% of hillslope area exceeds a 30° slope at the 10 and 1 m scales, respectively (Figure 3). This indicates that much of the terrain is steeper than the angle of repose, where existing ravel models are not applicable. Exhumation ages and catchment-averaged cosmogenic radionuclide exposure ages both indicate erosion rates in the San Gabriel Mountains ranging from 0.1 to 1 mm/yr, with erosion rates of ~0.5 mm/yr along the southern front [*Blythe et al.*, 2000; *Spotila et al.*, 2002; *DiBiase et al.*, 2010].

2.1. 2009 Station Fire

[10] We measured ravel accumulation 5 months after the cessation of the 2009 Station Fire in Haines Canyon, San Gabriel Mountains, California (Figure 2). Prior to the Station Fire, Haines Canyon burned in the 1975 Mill Fire. Although our measurements were made in February after winter rain, there was minimal modification (i.e., rilling or slumping) of the ravel cones as they showed angle of repose slopes. Measurements were made on a 500 m section of U.S. Forest Service road that was maintained prior to the fire and had little to no prefire ravel accumulation. We made measurements of ravel cone heights and lengths spaced every 1 m along the transect using a laser range finder. These were converted to volumes by assuming a 30° slope along the free faces of the cones and a prefire 70° angle between the road and the hillslope, as verified along transects devoid of ravel.

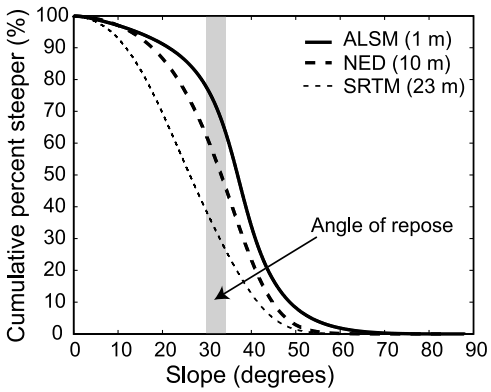

Figure 3. Cumulative probability distribution of topographic gradients within the San Gabriel Mountains at three different scales. Calculations were made for a 395 km^2 area of the southwestern San Gabriel Mountains (covering much of the extent shown in Figure 2) using Airborne Laser Swath Mapping data ("ALSM," 1 m resolution), the National Elevation Data set ("NED," 10 m resolution, U.S. Geological Survey), and the Shuttle Radar Topography Mission data ("SRTM," 23 m resolution, U.S. Geological Survey). ALSM-based slope data was sampled every hundredth pixel to manage data size. The shaded vertical area shows the approximate angle of repose for loose sediment.

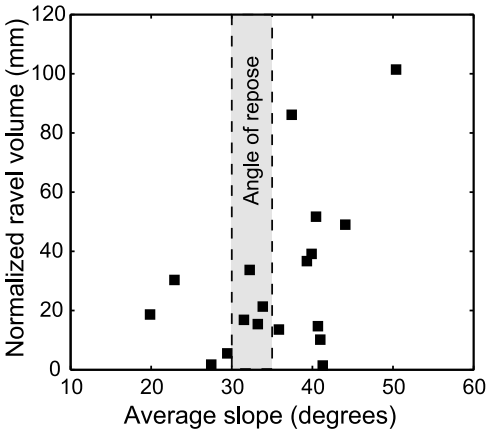

Figure 4. Measured ravel accumulation volumes per area of contributing hillslope versus the average gradient of the contributing hillslope. Ravel volumes were measured in February 2010 following the 2009 Station fire in Haines Canyon, California, along a 500 m stretch of U.S. Forest Service road. Contributing hillslope areas and slopes were measured using a 1 m resolution digital elevation model with data collected using airborne laser swath mapping. The shaded vertical area shows the approximate angle of repose for loose sediment.

[11] Hillslope areas contributing to the ravel deposits were measured using a 1 m resolution digital elevation model (DEM) generated from airborne laser swath mapping (ALSM) collected following the fire. The DEM revealed that the ravel-cone transect was fed by 18 separate subbasins with non-overlapping contributing hillslope areas that were mapped following paths of steepest decent.

[12] Results show net ravel yields over a 5 month period of 1 to 100 mm with an average value of 30 mm, a median of 20 mm, and a standard deviation of 27 mm (Figure 4). These yields were calculated by normalizing the accumulation volumes by the contributing area of the landscape (Figure 4). Although the results are variable, there appears to be an increase in dry ravel accumulation for cones with contributing basins that have average slopes greater than about 30°–35°, coincident with the angle of repose. This finding is consistent with the work of others. For example, *Gabet* [2003] observed an abrupt increase in ravel flux per unit width from ~0.2 kg/m yr to ~3 kg/m yr at a hillslope gradient of ~30°. Likewise, *Bennett* [1982] observed an abrupt increase in annual dry ravel yield from 2.9 mm/yr to 22.4 mm/yr at a similar hillslope angle.

2.2. Debris Basin Data

[13] Because of the San Gabriel Mountains' close proximity to communities, Los Angeles County has captured sediment in debris basins discharged from 115 southern catchments with drainage areas ranging from 0.02 to 7 km^2 (average of 1.2 km^2) since as early as the 1920s [*Rowe et al.*, 1954; *Los Angeles County Department of Public Works* (*L.A.C.D.P.W.*), 1991; *Lavé and Burbank*, 2004]. The San Gabriel debris basin data set is one of the longest-running records of sediment fluxes in steep mountain terrain prone to fires [*L.A.C.F.C.D.*, 1959; *L.A.C.D.P.W.*, 1991]. Nonetheless, extracting information about dry ravel from the data is difficult because the basins capture sediment generated and transported by a range of processes. Following fire, the majority of the increase in sediment flux is probably produced by dry ravel [*Krammes*, 1965; *Rice*, 1974, 1982; *Lavé and Burbank*, 2004], but other sediment sources exist including rilling, shallow landsliding, and evacuation of preexisting fluvial deposits by debris flows. Although many channels are inundated with ravel immediately following a fire (e.g., Figure 1a), this sediment is not flushed into debris basins until winter storms allow it to be transported by fluvial processes and debris flows. In lieu of a robust method to uniquely identify sediment produced by dry ravel, we treat the postfire sediment yield from the debris basins as a result of dry ravel and recognize that it should be considered an upper limit.

[14] To make comparisons across catchments of different sizes, we normalized the annual volumetric sediment flux for each debris basin by the area of the catchment upstream of the basin. In order to compare yields from different years (with different storm events), we multiplied each annual sediment flux record by $\overline{Q_w}/Q_w$ where Q_w is the annual-average daily water discharge for the year of interest and $\overline{Q_w}$ is the median annual average daily discharge over the record period. Since discharge data are not available for most catchments, we used the discharge of a major drainage within the study area, Arroyo Seco (U.S. Geological Survey gauge 11098000), which should serve as a good proxy for wet versus dry years. Thus, there is no account of the variability in precipitation for different catchments.

[15] The resulting normalized sediment yields are shown versus the time since the basins burned with no intervening fires (Figure 5). The number of data points decreases in time because there are very few examples of catchments with long durations in between fires. Although there is scatter in the data, they do reveal that the average sediment fluxes during the first 2 years following a fire are larger than later years, which are closer to background erosion rates of 0.1–1 mm/yr [*Blythe et al.*, 2000; *Spotila et al.*, 2002; *Lavé and Burbank*, 2004; *DiBiase et al.*, 2010]. The first year following fire has a production rate with a geometric mean of 8 mm/yr (and a range of 2 mm/yr to 36 mm/yr for different catchments), which is more than an order of magnitude larger than background rates. These results are consistent with *Lavé and Burbank* [2004], who analyzed the same data and showed that background erosion rates averaged 0.7–0.9 mm/yr when effects of fire were removed. This is encouraging because they used the same debris basin data, but employed an empirical model to account for the effects of fire rather than comparing sediment fluxes as a function of time since burned.

[16] The abrupt increase in postfire sediment yield as shown from debris basin data is consistent with other studies that focused exclusively on dry ravel. For example, *Bennett* [1982] showed that, at the base of burned hillslopes, 65% of the net sediment accumulation over a 2 year period was produced within the first 24 h following the burn, with 95% accumulated within 8 months of the fire. *Florsheim et al.* [1991] found that ravel accumulation was an order of magnitude smaller the second summer after a wildfire, as compared to the first. Likewise, *Jackson and Roering* [2009] found that ravel accumulation was imperceptible the second

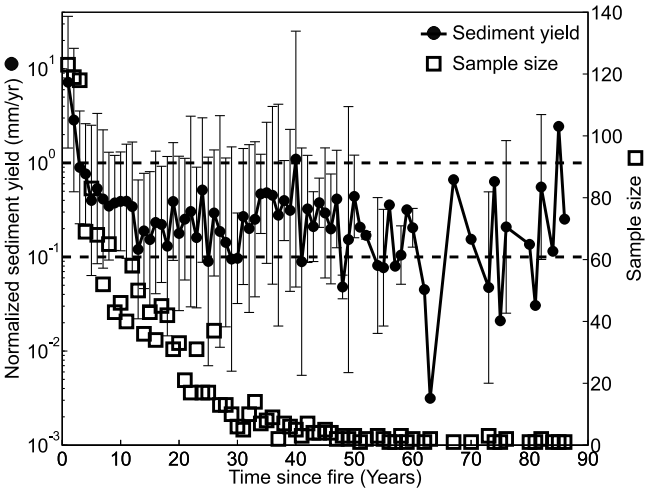

Figure 5. Annual sediment yield from 93 debris basins located along the southern front of the San Gabriel Mountains, California (Figure 2) as a function of time since a given wildfire (without any intervening fires). Annual debris basin volumes were normalized for the contributing area of the catchment (as reported by *L.A.C.P.D.W.* [1991]) and by a nondimensional precipitation factor to attempt to normalize wet and dry years (see text for details). Closed symbols represent geometric means for all catchments and all fires analyzed, and error bars represent plus and minus one geometric standard deviation. The "sample size" is the number of data points available for each time bin (open squares). Error bars are absent for time bins with only a single data point. The horizontal dashed lines bracket the approximate long-term erosion rate of the San Gabriel Mountains of 0.1 to 1 mm/yr (see text for details).

year following wildfire, as compared to a sediment yield of 2.5 mm/yr the first year.

3. Hypothesis and Model Formulation

[17] To explain these observations in postfire sediment yield, herein we present a mass balance model to predict ravel flux following fires due to the evacuation of sediment stored behind vegetation. We focus on building a model that can explain rapid postfire ravel yields that exceed background sediment yields by an order of magnitude for hillslopes with average gradients that exceed the angle of repose. The goal is to focus on the cause for the general trends in ravel-yield averages and not necessarily the variability in the data, although this is discussed in section 7.

[18] It has long been proposed that sediment flux following fires increases as a result of incineration of vegetation dams that temporarily sequester sediment on hillslopes [e.g., *Krammes*, 1965; *Swanson*, 1981; *Rice*, 1982; *Wells*, 1987]. For example, *Florsheim et al.* [1991] argued that vegetation can act as a dam, trapping loose sediment (Figures 1c and 6). At slopes greater than the angle of repose and in the absence of vegetation (or other perturbations in local slope caused by surface roughness), the sediment is unstable and will roll and bounce downslope until it reaches lower-gradient terrain. Fires can reduce the vegetation density (i.e., the number of plants per unit hillslope area) or the plants' capacity to impound sediment, thereby releasing sediment via dry ravel that would otherwise remain stored on steep hillslopes.

[19] Our goal is to quantitatively model sediment trapping and release by vegetation in the simplest way possible that still captures the appropriate physical processes. By mass conservation in one dimension, we set the change in thickness of inorganic sediment stored on a hillslope to the divergence of the volumetric sediment flux (Q) and the rate of bedrock to soil conversion (E) [e.g., *Dietrich et al.*, 2003], or

$$\frac{dh}{dt} = -\frac{1}{w}\frac{dQ}{dx} + \frac{\rho_r}{\rho_s}E, \tag{1}$$

where h is the thickness of loose sediment on the hillslope, w is the width of the hillslope, ρ_r and ρ_s are the bulk densities of bedrock and soil respectively, t denotes time, and x is the downslope coordinate (Figure 6). The total sediment flux via dry ravel reaching the base of a hillslope can be found by integrating equation (1) from the top of the hillslope $Q\,(x = 0) = 0$ to the base of the hillslope $Q\,(x = L) = \overline{Q}$ and assuming $E \neq f(x)$, which yields

$$\overline{Q} = \frac{\rho_r}{\rho_s}EA_b - \frac{dV}{dt}, \tag{2}$$

where $A_b = wL$ is the surface area of the hillslope, L is the length of the hillslope in the downslope direction, and V is the volume of sediment stored across that area. Following *Florsheim et al.* [1991] and others [e.g., *Krammes*, 1965; *Swanson*, 1981; *Rice*, 1982; *Wells*, 1987], we assume that sediment is stored on hillslopes with average gradients greater than the angle of repose because roughness created by vegetation (e.g., stems, branches, leaves and litter) locally forms pockets with shallower gradients (Figures 1c and 6). The

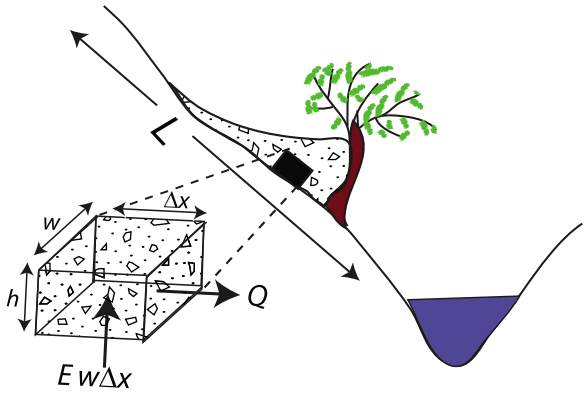

Figure 6. Mass balance for a sediment pile behind a vegetation dam where x is the downslope coordinate, L is the total hillslope length, w is the total hillslope width, h is the thickness of the sediment pile averaged over the hillslope area, Q is the downslope volumetric flux, and E is the soil production rate. This cartoon is meant to be a generic representation of sediment trapping by vegetation after *Florsheim et al.* [1991]. It does not depict trapping by low-lying branches or litter that may be important in some landscapes.

total volumetric capacity stored on hillslopes by vegetation dams can be written as

$$V_c = V_{ci} c A_b, \tag{3}$$

where V_{ci} is the volume of sediment stored behind each plant and c is the number of plants per unit area of land surface (i.e., the vegetation density).

[20] We allow for the possibility that $V < V_c$, which can result, for example, if there has not been enough time to fill the storage space behind vegetation to capacity. To calculate the actual sediment storage, we assume that if $V < V_c$, some volumetric fraction (ψ) of soil produced from bedrock is impounded by vegetation on the hillslope. We also assume that once trapped by vegetation dams, sediment is not lost due to factors other than fire such as disturbance by wind, earthquakes, or biota. With these assumptions, the rate of volumetric change of sediment stored behind vegetation is

$$\frac{dV}{dt} = \psi \frac{\rho_r}{\rho_s} E A_b \quad \text{for} \quad V < V_c \tag{4a}$$

$$\frac{dV}{dt} = \frac{dV_c}{dt} = A_b \frac{d(cV_{ci})}{dt} \quad \text{for} \quad V \geq V_c. \tag{4b}$$

In other words, if $V < V_c$ then the volumetric sediment storage increases in time at a rate proportional to the soil production rate and the contributing hillslope area. On the other hand, if $V \geq V_c$, then changes in volumetric sediment storage can only result through changes in the storage capacity. Fire can reduce storage capacity through decreasing the vegetation density (c) or the storage capacity of individual plants (V_{ci}), resulting in a pulse of sediment to the channel.

[21] The sediment yield (i.e, $\overline{Q}/A_b$) delivered by dry ravel to the base of a hillslope can be computed by combining equations (2) and (4) as

$$\frac{\overline{Q}}{A_b} = (1 - \psi) \frac{\rho_r}{\rho_s} E \quad \text{for} \quad V < V_c \tag{5a}$$

$$\frac{\overline{Q}}{A_b} = \frac{\rho_r}{\rho_s} E - \frac{d}{dt}(cV_{ci}) \quad \text{for} \quad V \geq V_c. \tag{5b}$$

Equation (5a) reduces to $\overline{Q} = 0$ if $\psi = 1$ because all sediment produced from bedrock is assumed to be captured behind vegetation for $V < V_c$. If $V \geq V_c$ and $\frac{d(cV_{ci})}{dt} = 0$ then equation (5b) predicts that all sediment is delivered to the base of the hillslope at a rate proportional to the soil production rate (E) and the hillslope area (A_b). The total flux can be higher or lower than this if $\frac{d(cV_{ci})}{dt} \neq 0$, which can result from vegetation growth or destruction by fire, for example.

4. Model Parameterization

[22] To explore the model, it is useful to use an example case study to parameterize the constants and variables. Here we focus on the southern front of the San Gabriel Mountains, California (Figure 2), because wildfires and associated large sediment fluxes are common and well documented [e.g., *Anderson et al.*, 1959; *Krammes*, 1965; *Lavé and Burbank*, 2004].

4.1. Soil Production Rates

[23] As discussed above, exhumation ages, catchment-averaged cosmogenic radionuclide exposure ages, and debris basin data all indicate long-term erosion rates in the San Gabriel Mountains ranging from 0.1 to 1 mm/yr, with erosion rates of ~0.5 mm/yr along the southern front [*Blythe et al.*, 2000; *Spotila et al.*, 2002; *Lavé and Burbank*, 2004; *DiBiase et al.*, 2010] (Figure 5). Catchment-averaged erosion rates, debris basin data, and exhumation rates incorporate processes (e.g., deep seated landslides, rockfall) that might not contribute to rejuvenation of sediment piles behind vegetation following wildfires. A more appropriate measure of sediment production rates comes from cosmogenic radionuclide exposure of soils in the San Gabriel Mountains. Maximum soil production rates occur on hillslopes where the soil mantle approaches zero thickness [*Heimsath et al.*, 1997, 2001], which is characteristic of the steep bedrock slopes of concern here. Available data in the San Gabriel Mountains for thin soil mantles indicate a maximum soil production rate of $E = 0.4$ mm/yr [*Heimsath*, 1999]. Although we favor this rate for our case study, we explore the model sensitivity to soil production rates ranging from 10^{-2} to 10^{0} mm/yr. In all cases, the bulk density of the rock and soil are assumed to be 2650 and 1590 kg/m^3, the latter of which corresponds to a soil porosity of 40%.

[24] The least-constrained parameter in the model is the fraction of soil produced from bedrock that is trapped by vegetation dams (ψ). The trapping efficiency might scale with the vegetation density and vegetation type; however, we currently have no data to justify a specific relationship for ψ. The fact that debris basins in the San Gabriel Mountains show finite sediment yields long after fire suggests that ψ is nonzero. We explore model sensitivity to ψ by varying it from 25% to 100%.

4.2. Fire Recurrence Interval

[25] Wildfires are common in the San Gabriel Mountains in summer months [*Wells*, 1981]. To quantify the historic fire recurrence interval, we analyzed U.S. Forest Service data [*United States Department of Agriculture Forest Service (U.S.D.A.F.S.)*, 2009] for the spatial extent of wildfires in the San Gabriel Mountains from 1901 to 2009 (including the extensive 2009 Station Fire). Ninety-three catchments along the southern front range were identified with a history of wildfire that contain debris basins. By overlaying the catchment boundaries with the spatial extent of fires, the percentage burned was estimated for each catchment during each fire. This allowed us to calculate the fire recurrence interval for subsets of the basins that had two subsequent fires that burned some threshold proportion of the catchment area. The results show that in the past century, individual catchments have had mean fire recurrence intervals (t_{fire}) ranging from about 22 to 37 years (Figure 7), with the longer recurrence intervals corresponding to basins that nearly completely burned in two subsequent fires. These calculations are similar to the findings of others [*Swanson*, 1981; *Lavé and Burbank*, 2004]; however, natural recurrence intervals were likely longer (~100 years) prior to human development

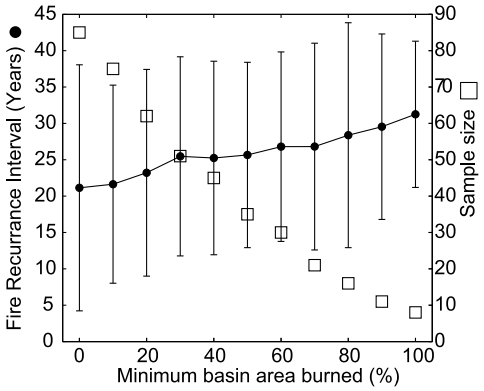

Figure 7. Mean recurrence interval (black dots) plus/minus one standard deviation (error bars) of documented wildfires in the San Gabriel Mountains, California, spanning 1901 to 2009 for the 93 catchments analyzed in section 2.2. Different recurrence intervals are shown for subsets of the database where only basins with a minimum percentage of burned landscape were included in the sample population (open squares). Recurrence interval was calculated using the Weibull method. The date and spatial extent of fires were obtained from the U.S. Forest Service [*U.S.D.A.F.S.*, 2009].

[*Lavé and Burbank*, 2004]. Since we will compare the model to historical data, we set t_{fire} = 35 years.

4.3. Vegetation Recovery

[26] To implement the model, we need to specify the volumetric capacity of vegetation to impound sediment (V_c) as a function of time since a fire. The postfire response of vegetation density may depend on a number of factors including, for example, plant size [e.g., *Zammit and Zedler*, 1992] and the degree to which plant roots burn during a fire, with a more severe burn potentially requiring seeding for reestablishment [e.g., *Shakesby and Doerr*, 2006]. In addition, the temporal response of V_{ci} to fire might depend on the establishment of low-lying branches and leaf litter to aid in trapping loose sediment, for example. Like plants, it is sensible that the sediment piles should reach an upper limit in size (i.e., sediment cannot be sequestered on hillslopes indefinitely). This is especially true given the steep slopes considered here and the fact that debris-basin sediment-yield data match the background soil production rate after approximately 10 years since a burn (Figure 5). Because little quantitative information exists to justify a more complicated response function for V_c, here we opt for a simple closure using a logistic equation which characterizes the disturbance response of many biological systems [e.g., *Grime and Hunt*, 1975; *Berryman*, 1992].

$$V_c = \left(V_{c0} - V_{cf}\right)\left(1 - \exp\left(-\frac{t}{t_{veg}}\right)\right) + V_{cf}, \qquad (6)$$

where V_{c0} is the undisturbed sediment storage capacity of vegetation, V_{cf} is the residual storage capacity unrelated to fire or vegetation (e.g., due to bedrock roughness), and t_{veg} is the characteristic timescale of sediment-storage response as dictated by vegetation regrowth. Although relationships alternative to equation (6) could be proposed, we show in section 6 that the predicted ravel yield is rather insensitive to the functional form of equation (6), as long as t_{veg} is small.

[27] Most of the vegetation in the catchments of interest is chaparral (e.g., *Adenostoma fasciculatuni*, *Quercus dumosa*, *Garrya veatchii*, *Heteromeles arbutifolia*, *Arctostaphylos glauca*, *Ceanothus crassifolius*, *Prunus ilicifolia* [*Keeley*, 1992; *U.S.D.A.F.S.*, 2009]). Field data in the San Gabriel Mountains shows that it takes about 5 years for ~80% of the chaparral to reestablish following fire [*L.A.C.D.P.W.*, 1991]. Following equation (6), this corresponds to a characteristic timescale for vegetation response to fire of $t_{veg} \approx 3$ years. If sediment storage also depends on reestablishment of litter, the characteristic timescale might be longer than t_{veg} = 3 years; however, litter piles are often small on slopes exceeding the angle of repose. In the model simulations, we assume t_{veg} = 3 years and also explore model sensitivity to longer vegetation response timescales of t_{veg} = 10, 30 and 50 years.

[28] To apply equation (6), we need to specify the sediment storage capacity of an undisturbed vegetated hillslope per unit area (V_{c0}/A_b). Following equation (3), V_{c0}/A_b can be estimated from the product of the volume of sediment stored by each individual plant (V_{c0i}) and the vegetation density (c_0) for hillslopes that have completely recovered from disturbance. To our knowledge, data does not exist for the capacity of individual plants to store sediment. We made rough visual estimates of sediment piles exposed after fire on slopes approaching the angle of repose in the San Gabriel Mountains and found sediment pile dimensions of ~0.2 m high, ~0.2 m wide, and ~0.5 m long, or $V_{ci} \approx 0.02$ m^3 (Figure 1c). Ideally estimates should be made on slopes exceeding the angle of repose prior to fire in a landscape where sediment piles are known to be at capacity, but these measurements are inherently difficult due to the steep slopes, vegetation cover, and the temporal monitoring required to test for at-capacity conditions. Our postfire estimates should be reasonable approximations because estimates were made on slopes slightly less than the angle of repose so that the soil mantle was thin, but sediment piles remained immediately following the fire. Fortunately, systematic fieldwork has been performed to constrain undisturbed vegetation density in the San Gabriel Mountains, where c_0 = 0.5 plants/m^2 [*Keeley*, 1992]. Combining these two values results in an estimate for V_{c0}/A_b of 10 mm. We explore model sensitivity to V_{c0}/A_b by varying it between 1 and 20 mm. For all model simulations we assume V_{cf} = 0 for simplicity, although it is likely nonzero (and may decreases as a function of hillslope gradient) due to bedrock roughness that can create local pockets for sediment accumulation even on hillsides with average gradients that exceed the angle of repose.

5. Model Results

[29] Model results are shown in a series of four figures (Figures 8–11) where all parameters are held constant at the values specified above for the San Gabriel Mountains and E = 0.4 mm/yr, ψ = 0.5, V_{c0}/A_b = 10 mm, and t_{veg} = 3 years, except in Figure 8 where E is varied, Figure 9 where ψ is varied, Figure 10 where V_{c0}/A_b is varied, and Figure 11 where t_{veg} is varied.

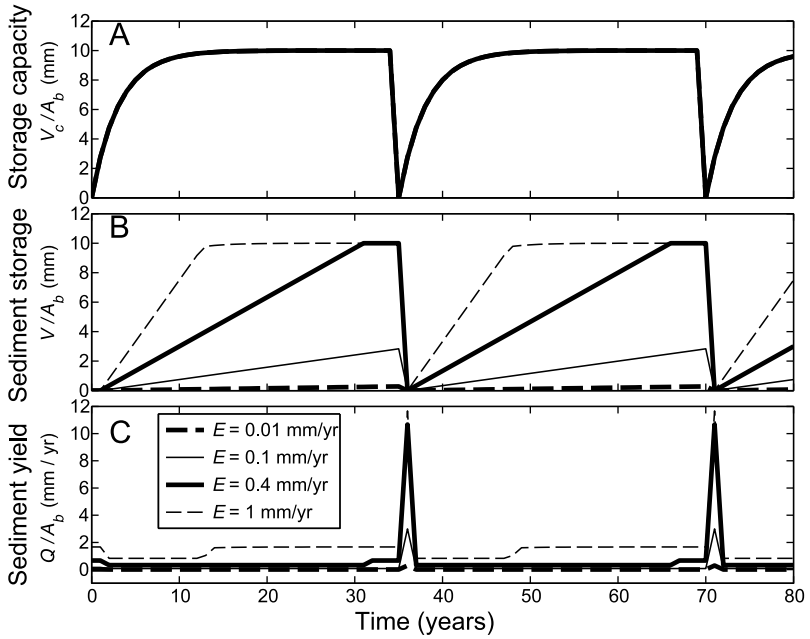

Figure 8. Model simulation for the San Gabriel Mountains, California, showing (a) the vegetation storage capacity, (b) the sediment storage on the hillslope, and (c) the average annual sediment yield at the base of the hillslope as a function of time and soil production rate, E. The storage capacity goes to zero when a wildfire occurs; ψ is 0.5, V_{c0}/A_b is 10 mm, and t_{veg} is 3 years. See text for other model inputs.

[30] Model results show that the drop in vegetation storage capacity due to fire causes a release of sediment to the channel at the hillslope base (Figure 8). For the parameters specified and E = 0.4 mm/yr, this gives a pulse of ~10 mm of sediment yield, which, when averaged over a year, is 25 times greater than the imposed background soil production rate, and is similar to field observations [e.g., *Rice*, 1982]. Following the fire, it takes ~10 years for the vegetation to

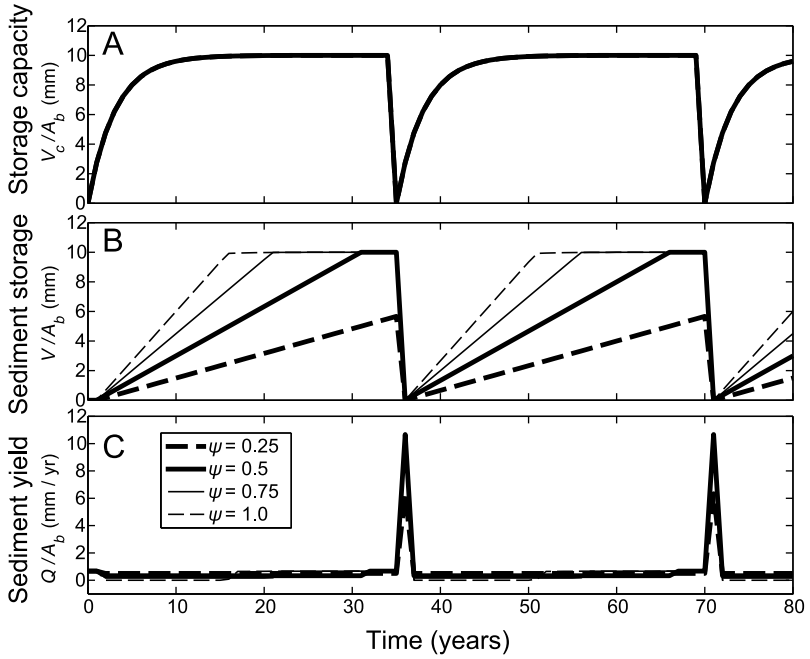

Figure 9. Model simulation for the San Gabriel Mountains, California, showing (a) the vegetation storage capacity, (b) the sediment storage on the hillslope, and (c) the average annual sediment yield at the base of the hillslope as a function of time and trapping efficiency, ψ. The storage capacity goes to zero when a wildfire occurs; E is 0.4 mm/yr, V_{c0}/A_b is 10 mm, and t_{veg} is 3 years. See text for other model inputs.

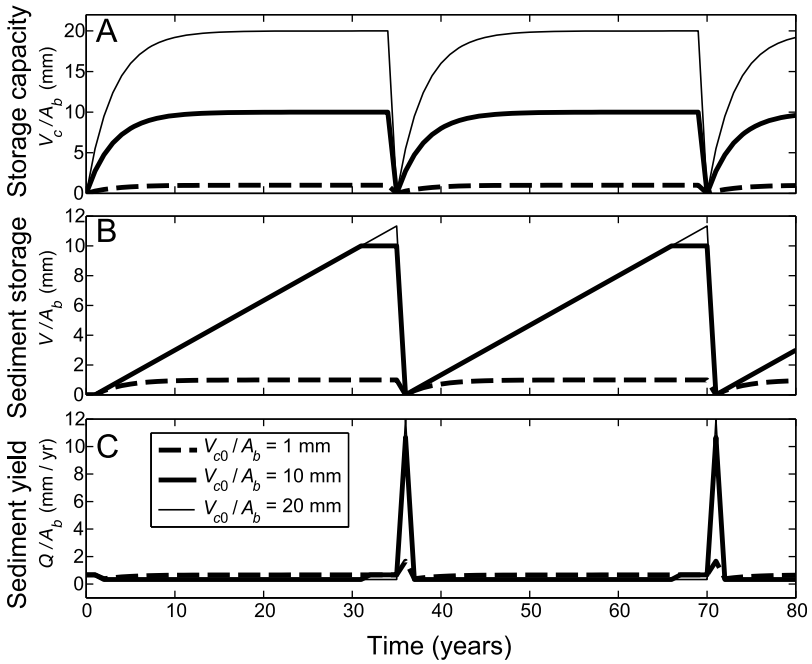

Figure 10. Model simulation for the San Gabriel Mountains, California, showing (a) the vegetation storage capacity, (b) the sediment storage on the hillslope, and (c) the average annual sediment yield at the base of the hillslope as a function of time and undisturbed sediment-storage capacity of the vegetation, V_{c0}/A_b. The storage capacity goes to zero when a wildfire occurs; E is 0.4 mm/yr, ψ is 0.5, and t_{veg} is 3 years. See text for other model inputs.

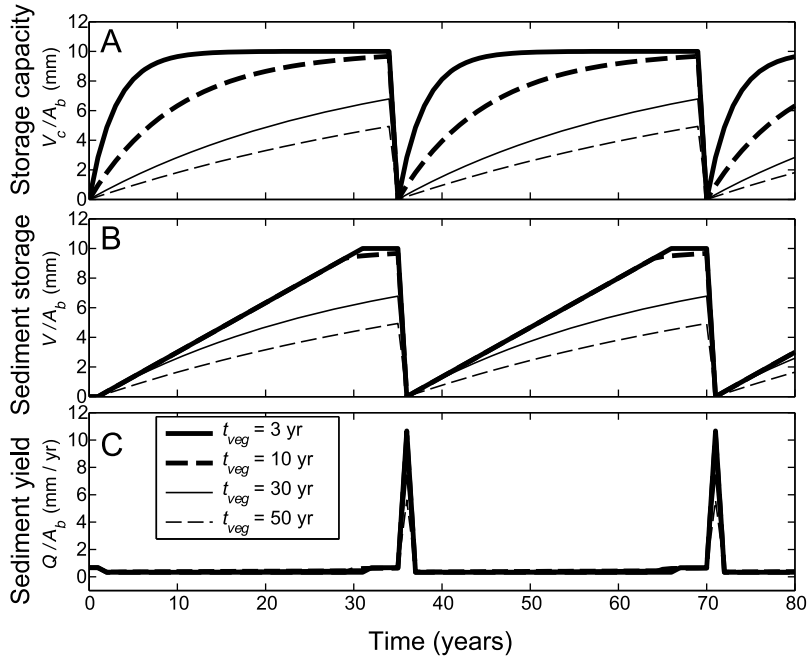

Figure 11. Model simulation for the San Gabriel Mountains, California, showing (a) the vegetation storage capacity, (b) the sediment storage on the hillslope, and (c) the average annual sediment yield at the base of the hillslope as a function of time and vegetation recovery timescale, t_{veg}. The storage capacity goes to zero when a wildfire occurs; E is 0.4 mm/yr, ψ is 0.5, and V_{c0}/A_b is 10 mm. See text for other model inputs.

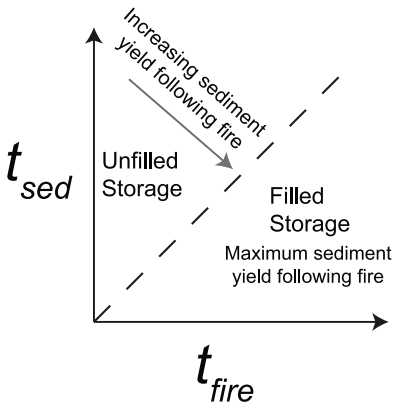

Figure 12. Recovery timescale of a hillslope to replenish sediment storage (t_{sed}) versus the recurrence interval of wildfire (t_{fire}) for the case when vegetation regrowth does not limit sediment storage (i.e., $t_{veg} \ll t_{fire}$). When $t_{fire} > t_{sed}$ the hillslope is at its maximum storage capacity and the postfire sediment flux response is insensitive to the rate of soil production or fire recurrence interval. When $t_{fire} < t_{sed}$ unfilled storage exists on the hillslope and the postfire sediment flux response is a function of soil production rate and time since the last burn.

regrow to its prefire state (Figure 8a). However, it takes much longer, 30 years, for the sediment reservoirs behind the vegetation to return sediment loads to their prefire state (Figure 8b). During this period, the model predicts that sediment yields to channels will be reduced to 50% of the long-term rate (or 0.2 mm/yr) due to sediment capture by vegetation given the assigned value of $\psi = 0.5$ (Figure 8c).

[31] With all other parameters held constant, a heightened soil production rate has no effect on the sediment yield following wildfire (Figure 8c). This is because the fire recurrence interval is sufficiently long that, prior to a subsequent fire, the vegetation has fully recovered and the sediment reservoirs have completely refilled. Thus, the increased soil production rate only decreases the timescale for the vegetation dams to refill (Figure 8b) and increases the sediment yield during nonfire periods. The same reasoning holds for the trapping efficiency where fire-induced sediment yield is insensitive to trapping efficiency as long as ψ is greater than ~40% (Figure 9b). However, for soil production rates smaller than ~0.2 mm/yr (and $\psi = 0.5$) or $\psi < 40\%$ (and $E = 0.4$ mm/yr), vegetation dams are predicted to be under capacity with respect to sediment during wildfire (Figures 8b and 9b) given the other parameters specified (e.g., $t_{fire} = 35$ years). This results in smaller sediment yields following fire and a sediment yield dependency on E, ψ, and the time elapsed since the last fire (Figures 8c and 9c).

[32] Because the model suggests that the vegetation dams in the San Gabriel Mountains should be at capacity at the time of wildfire, the specific value of the undisturbed sediment-storage capacity has a strong influence on fire-induced sediment yield (Figure 10). In particular, the volume of sediment stored behind vegetation and the fire-induced sediment yield are both equal to V_{c0}/A_b for $V_{c0}/A_b < 12$ mm because there is sufficient time in between fires to fill the vegetation dams to capacity. For example, if $V_{c0}/A_b = 1$ mm, then only 1 mm of additional sediment yield is available following wildfire (Figure 10). On the other hand, if $V_{c0}/A_b > 12$ mm then the reservoirs are too large to be filled in the time between fires with the given soil production rate (Figure 10). Thus, for $V_{c0}/A_b > 12$ mm, the postfire sediment yield is supply limited and is a function of time since the last fire, E and ψ, rather than V_{c0}/A_b.

[33] In all cases discussed above, the vegetation response timescale was small compared to the fire recurrence interval such that the vegetation regrowth played no role in fire-induced sediment yield. Although field data on vegetation recovery indicate this is a robust result for the San Gabriel Mountains [*L.A.C.D.P.W.*, 1991], it is useful to explore variable vegetation response timescales for other landscapes where vegetation response might be slower. Model results show that there is little difference in the predicted postfire sediment yield for $t_{veg} = 3$ years and 10 years as the vegetation is still able to reestablish between fires (Figure 11). However, for $t_{veg} = 30$ years and 50 years, the vegetation does not regrow fully before the subsequent fire and consequently the storage capacity never reaches its undisturbed value (i.e., $V_c \neq V_{c0}$). This results in a reduction in fire-induced sediment yield and a dependency of sediment yield on the time since the last fire and t_{veg}.

6. Timescale Analysis

[34] The model scenarios and sensitivity analyses in section 5 illustrate that the fire-induced sediment yield can depend on different variables depending on the vegetation regrowth timescale (t_{veg}), the fire recurrence timescale (t_{fire}) and the time to fill the sediment accommodation space to capacity (t_{sed}). The latter timescale can be found by combining equations (5a) and (5b) and integrating with respect to time as,

$$t_{sed} = \frac{V_c}{\psi \frac{\rho_r}{\rho_s} E A_b}. \tag{7}$$

Here we use these timescales to outline the expected enhanced sediment yield following fires for a generic landscape.

[35] When $t_{sed} > t_{fire}$ there is unfilled vegetation-dam storage space. In this case, the volume of sediment stored on the hillslope just prior to fire (i.e., $t \approx t_{fire}$) can be found by integrating equation (4a) as

$$V = \psi \frac{\rho_r}{\rho_s} E A_b t_{fire} \quad \text{for} \quad t_{sed} > t_{fire}. \tag{8}$$

Thus, the volume of sediment stored on a hillslope that can contribute to fire-induced sediment yield is a function of the soil production rate and the fire recurrence interval (Figure 12). It is independent of the capacity of the vegetation to store sediment (V_c), but remains a function of the sediment trapping efficiency (ψ).

[36] Alternatively if $t_{sed} < t_{fire}$ then the volume stored on a hillslope just prior to fire depends only on the vegetation sediment-storage capacity (Figure 12). From equation (6), if

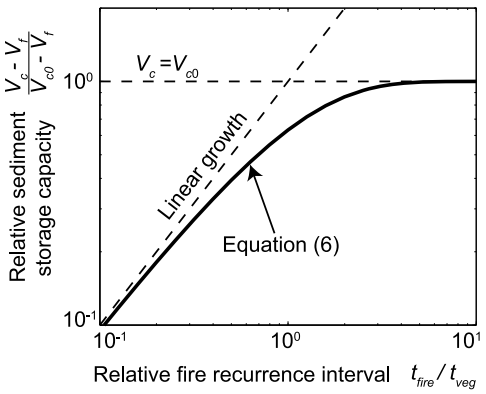

Figure 13. Relative volumetric capacity of vegetation to store sediment on a hillslope at the time of fire versus the fire recurrence interval normalized by the vegetation regrowth timescale following equation (6). Also shown are the end-member cases of $V_c = V_{c0}$ for $t_{fire} > t_{veg}$ and linear growth for $t_{fire} \ll t_{veg}$.

the vegetation recovery is relatively rapid (i.e., $t = t_{fire} > t_{veg}$) then the volume of sediment stored just prior to fire is given by

$$V = V_c \approx V_{c0} \quad \text{for} \quad t_{fire} > t_{veg} \quad \text{and} \quad t_{sed} < t_{fire}. \tag{9}$$

In other words, the sediment yield due to fire is independent of t_{fire}, E and ψ, and instead is solely a function of the undisturbed vegetation sediment-storage capacity. This is the case for maximum postfire sediment yield (Figure 12).

[37] A third scenario exists for the case where vegetation regrowth limits sediment storage. Again, following equation (6), this occurs for $t = t_{fire} < t_{veg}$. For the case where $t_{fire} \ll t_{veg}$, equation (6) can be approximated though Taylor expansion as

$$V = V_c \approx V_{c0} \frac{t_{fire}}{t_{veg}} \quad \text{for} \quad t_{fire} \ll t_{veg} \quad \text{and} \quad t_{sed} < t_{fire}. \tag{10}$$

Thus, the volume of sediment stored is linearly dependent on the undisturbed-vegetation sediment-storage capacity, fire recurrence interval and the inverse of the vegetation regrowth timescale (Figure 13), and is independent of E and ψ.

7. Comparison to Field Data

[38] For the parameters specified, the model can explain the approximate order of magnitude increase in ravel yield immediately following a fire observed both in measurements of individual hillslopes (e.g., Figure 4) and debris basin data (Figure 5). For example, from the debris basin data, the first year following fire has sediment yield of 8 mm/yr (with a range of 2 mm/yr to 36 mm/yr for different catchments), which is more than an order of magnitude larger than background rates and roughly consistent with our model predictions of ~10 mm/yr of ravel yield (Figure 8).

[39] The scatter in ravel measurements is significant, however, and it is not unlike previous observations. For example, during the first dry season following wildfire in the San Gabriel Mountains, ravel yields on slopes with average gradients that exceed 30° have been reported to be 2.7 mm [*Krammes*, 1965], 3.9 mm [*Rice*, 1982] and 185 mm [*Doehring*, 1968]. If the vegetation dams are indeed at sediment storage capacity, the model suggests that the natural variability could be a result of variations in vegetation density, vegetation type, ψ, t_{veg}, and the sediment-storage capacity of individual plants within each catchment.

[40] An average annual sediment yield was calculated in the model simulations because this was most useful for comparing to the annual debris basin yield measurements and annual ravel yields reported by others. It is important to note, however, that the model predicts that all fire-induced sediment yield occurs immediately following loss of hillslope storage capacity, which might occur in a matter of hours or days following fire. Thus, our predicted annual-average postfire ravel yield of 10 mm may in fact be released over a few days (at a rate two orders of magnitude greater than annual-average postfire ravel yield and three orders of magnitude greater than the soil production rate). This rapid delivery and subsequent rapid decline of ravel yield is consistent with the measurements of *Bennett* [1982], who showed that most of the annual net ravel yield occurred within the first 24 h of a fire. Although a decline in ravel yield with time since wildfire has previously been attributed to rejuvenation of vegetation, a coarse sediment lag or litter cover that protects the soil [*Shakesby and Doerr*, 2006], we suspect that, at least on the steep slopes considered here, it is due to a reduction in the availability of unstable particles either because of complete stripping of the soil mantle or because remaining particles migrate to stable locations (e.g., due to roughness induced by bedrock or burned vegetation, i.e., $V_{cf} \neq 0$). This is consistent with the observations of *Jackson and Roering* [2009] of large patches of bedrock that were freshly exposed following wildfires in Oregon.

[41] Our model also explains the abrupt increase in dry ravel flux observed for average slopes greater than the angle of repose [e.g., *Bennett*, 1982; *Gabet*, 2003; *Jackson and Roering*, 2009] (Figure 4). At these slopes sediment is gravitationally unstable, and the loss of roughness and reduced local steepness provided by vegetation and litter results in rapid particle transport [*Gabet*, 2003; *Roering and Gerber*, 2005]. Natural hillslopes are not smooth, however. Bedrock roughness likely traps less sediment with increasing slope (i.e., V_{cf} likely decreases with increasing slope), indicating the need to route ravel down hillslopes, perhaps similar to water-routing algorithms.

[42] Unlike the model predictions (Figure 8), the debris basin data do not show reduced sediment yields in the decade following the fire (Figure 5). This might be because the debris basins integrate other sources of sediment in addition to dry ravel that are not taken into account in the model (e.g., overland flow erosion, gullying, shallow landslides). Moreover, some postfire sediment is temporarily stored in channels as ravel cones or fluvial deposits and may not be completely evacuated in the first year following the fire. This may explain why sediment fluxes into debris basins remain high for 2 or 3 years following a fire (Figure 5), whereas ravel fluxes taper abruptly within the first year [e.g., *Bennett*, 1982].

8. Discussion

[43] One of the most significant differences between our model and previous work is that we assume that fire does

not influence the rate of soil production, and instead affects the timescale of storage and release of loose material on the hillslopes. Thus, in our model, fire does not alter the bedrock erosion rate or landscape form over geomorphic timescales. This is counter to the work of *Lavé and Burbank* [2004], who argued that erosion due to fire can be added or subtracted from the "nonfire" erosion rate. *Swanson* [1981] also suggested that fire causes a pulse of sediment flux that supplements the background sediment flux, such that the fire-induced load is not compensated by a reduced flux in subsequent years, as occurs in our model [see also *Rice*, 1982]. Likewise, *Roering and Gerber* [2005] argued that more frequent fires can alter the shape of hillslopes by changing the soil flux over geomorphic timescales.

[44] In addition to simply changing sediment storage on hillslopes, there are reasons to believe that fire could change the rate of soil production: through changing soil thickness, which can affect soil production rates [e.g., *Heimsath et al.*, 2001]; by shattering rock due to heat [*Shakesby and Doerr*, 2006]; or repeated cycles of root regrowth, for example. But it is unlikely that soil-production mechanisms, which rarely achieve rates greater than 1 mm/yr in the western U.S.A. [e.g., *Heimsath*, 1999; *Heimsath et al.*, 2001], can explain sediment yields of tens of millimeters within hours or days following wildfire. We argue that the increased sediment yield by orders of magnitude following fires results instead from loss of storage on steep hillslopes. It is clear that future work is needed to investigate changes in the rate of soil production from bedrock (if any) to explore the long-term geomorphic significance of fires in steep landscapes.

[45] We believe that, despite its simplicity, our sediment storage model provides a useful quantitative framework to predict ravel fluxes in response to fire on steep slopes. Given the necessary input parameters, the model could be used in different landscapes to predict sediment loading in channels and the potential for debris flows [e.g., *Cannon*, 2001; *Gartner et al.*, 2008; *Santi et al.*, 2008]. In addition to drainage area, burn intensity, and landscape steepness, which are used in existing statistical models for postfire sediment yield [*Cannon et al.*, 2010], our model points to the need to characterize the vegetation density and sediment-storage capacity, and in cases incorporate fire history, soil production rate and vegetation regrowth rate. The mass-conservation approach used herein may allow the model to be applied to landscapes in different climatic, geologic and tectonic settings, rather than relying on different statistical regressions for different regions.

[46] Despite the potential utility of the ravel model, its application requires specifying several poorly known parameters. Future work is needed to characterize the trapping ability of vegetation as a function of vegetation type and density. In addition, future work is needed to measure the volume of sediment stored by vegetation on steep slopes and explore their organic components and dependencies on vegetation size and type, sediment size distributions, and hillslope gradient.

9. Conclusions

[47] A quantitative model is proposed for postfire sediment yield by dry ravel on steep hillslopes as a result of the loss of capacity of vegetation to impound loose sediment. A mass balance framework is developed to quantify the storage of sediment on steep hillslopes as a function of the storage capacity of individual plants, vegetation density, and contributing hillslope area. Because loose sediment is gravitationally unstable on slopes greater than the angle of repose, the model predicts a sudden increase in sediment yield from steep hillslopes to channels following wildfire due to loss of vegetation that otherwise creates local shallow gradients. After a fire, time is required to reestablish vegetation and replenish hillslope storage of loose material, which introduces vegetation regrowth rate, soil production rate, and fire recurrence interval as important variables in controlling ravel flux depending on their relative characteristic timescales. The model explains the sudden pulse of sediment flux observed immediately following fires and the significant increase in sediment flux observed on slopes greater than ~30°–35°.

[48] For the case of the San Gabriel Mountains, the model predicts that postfire ravel yield is determined by the capacity of hillslope vegetation to impound sediment and the vegetation density. The fire recurrence interval is sufficiently long, such that vegetation is predicted to be fully reestablished and hillslope storage is at capacity prior to most wildfires; this renders the fire-induced ravel yield independent of the soil production rate, vegetation regrowth rate, and fire recurrence interval. The model prediction of an annual-average postfire ravel yield of ~10 mm/yr is within the range of normalized sediment yield measured from debris basins for the first year following wildfire 2 to 36 mm/yr (geometric mean of 8 mm/yr) and from direct ravel measurements following the 2009 Station Fire that range from 1 to 100 mm (median of 20 mm) measured over 5 months. The natural variability in ravel yields is most likely due to spatial variability in vegetation density and the sediment trapping capacity of vegetation which are not represented in the model simulations.

[49] In contrast to other models which assume that wildfire enhances sediment production from bedrock and therefore accelerates landscape evolution, our model shows that postfire sediment yields can be explained by wildfire-induced release of stored hillslope sediment with no contribution from heightened soil production.

[50] **Acknowledgments.** Funding for the work was provided by NSF EAR-0922199 grant to M.P.L. and the California Institute of Technology. The digital topographic data was collected by the National Center for Airborne Laser Mapping. Parts of the research presented were completed as part of Ge126 at Caltech, and the authors are grateful to class participants Janet Harvey, Mariya Levina, Ben Mackey, and Will Steinhardt. We thank Mike Oxford for facilitating access to the U.S. Forest Service records on wildfire history in the San Gabriel Mountains and Youssef Chebabi and Los Angeles County for providing debris basin data. Jerome Lavé kindly provided data compiled from his 2004 study. We are grateful to Sue Cannon, Jon Stock, Kevin Schmidt, and Jon Wilson for informal discussions and advice. Two reviewers and the Editor provided valuable comments that strengthened the final manuscript.

References

Anderson, H. W., G. B. Coleman, and P. J. Zinke (1959), Summer slides and winter scour: Dry-wet erosion in southern California, *Tech. Rep. PSW-36*, 12 pp., U. S. For. Serv. Pac. Southwest For. Range Exp. Stn., Berkeley, Calif.

Benda, L., and T. Dunne (1997), Stochastic forcing of sediment routing and storage in channel networks, *Water Resour. Res.*, *33*(12), 2865–2880, doi:10.1029/97WR02387.

Bennett, K. A. (1982), Effects of slash burning on surface soil erosion rates in the Oregon Coast Range, M. S. thesis, Oreg. State Univ., Corvallis.
Berryman, A. A. (1992), The origins and evolution of predator-prey theory, *Ecology*, *73*(5), 1530–1535, doi:10.2307/1940005.
Blythe, A. E., D. W. Burbank, K. A. Farley, and E. J. Fielding (2000), Structural and topographic evolution of the central Transverse Ranges, California, from apatite fission-track, (U-Th)/He and digital elevation model analyses, *Basin Res.*, *12*(2), 97–114, doi:10.1046/j.1365-2117.2000.00116.x.
Cannon, S. H. (2001), Debris-flow generation from recently burned watersheds, *Environ. Eng. Geosci.*, *7*(4), 321–341.
Cannon, S. H., J. E. Gartner, M. G. Rupert, J. A. Michael, A. H. Rea, and C. Parrett (2010), Predicting the probability and volume of postwildfire debris flows in the intermountain western United States, *Geol. Soc. Am. Bull.*, *122*(1–2), 127–144, doi:10.1130/B26459.1.
Coffman, G. C., R. F. Ambrose, and P. W. Rundel (2010), Wildfire promotes dominance of invasive giant reed (*Arundo donax*) in riparian ecosystems, *Biol. Invasions*, *12*(8), 2723–2734, doi:10.1007/s10530-009-9677-z.
DiBiase, R. A., K. X. Whipple, A. M. Heimsath, and W. B. Ouimet (2010), Landscape form and millennial erosion rates in the San Gabriel Mountains, CA, *Earth Planet. Sci. Lett.*, *289*(1–2), 134–144, doi:10.1016/j.epsl.2009.10.036.
Dietrich, W. E., D. Bellugi, L. Sklar, J. D. Stock, A. M. Heimsath, and J. J. Roering (2003), Geomorphic transport laws for predicting landscape form and dynamics, in *Prediction in Geomorphology*, *Geophys. Monogr. Ser.*, vol. 135, edited by P. Wilcock, and R. Iverson, pp. 103–132, AGU, Washington, D. C.
Doehring, D. O. (1968), The effect of fire on geomorphic processes in the San Gabriel Mountains, California, *Contrib. Geol.*, *7*(1), 43–66.
Eaton, E. C. (1935), Flood and erosion control problems and their solution, *Trans. Am. Soc. Civ. Eng.*, *101*, 1302–1330.
Eaton, B. C., C. A. E. Andrews, T. R. Giles, and J. C. Phillips (2010), Wildfire, morphologic change and bed material transport at Fishtrap Creek, British Columbia, *Geomorphology*, *118*(3–4), 409–424, doi:10.1016/j.geomorph.2010.02.008.
Florsheim, J. L., E. A. Keller, and D. W. Best (1991), Fluvial sediment transport in response to moderate storm flows following chaparral wildfire, Ventura County, southern California, *Geol. Soc. Am. Bull.*, *103*(4), 504–511, doi:10.1130/0016-7606(1991)103<0504:FSTIRT>2.3.CO;2.
Furbish, D. J., M. W. Schmeeckle, and J. J. Roering (2008), Thermal and force-chain effects in an experimental, sloping granular shear flow, *Earth Surf. Processes Landforms*, *33*(13), 2108–2117, doi:10.1002/esp.1655.
Gabet, E. J. (2003), Sediment transport by dry ravel, *J. Geophys. Res.*, *108*(B1), 2049, doi:10.1029/2001JB001686.
Gabet, E. J., and T. Dunne (2003), A stochastic sediment delivery model for a steep Mediterranean landscape, *Water Resour. Res.*, *39*(9), 1237, doi:10.1029/2003WR002341.
Gamradt, S. C., and L. B. Kats (1997), Impact of chaparral wildfire-induced sedimentation on oviposition of stream-breeding California newts (*Taricha torosa*), *Oecologia*, *110*(4), 546–549, doi:10.1007/s004420050193.
Gartner, J. E., S. H. Cannon, P. M. Santi, and V. G. Dewolfe (2008), Empirical models to predict the volumes of debris flows generated by recently burned basins in the western US, *Geomorphology*, *96*(3–4), 339–354, doi:10.1016/j.geomorph.2007.02.033.
Grime, J. P., and R. Hunt (1975), Relative growth-rate: Its range and adaptive significance in a local flora, *J. Ecol.*, *63*(2), 393–422, doi:10.2307/2258728.
Heimsath, A. M. (1999), The soil production function, Ph.D. thesis, Univ. of Calif., Berkeley.
Heimsath, A. M., W. E. Dietrich, K. Nishiizumi, and R. C. Finkel (1997), The soil production function and landscape equilibrium, *Nature*, *388*, 358–361, doi:10.1038/41056.
Heimsath, A. M., W. E. Dietrich, K. Nishiizumi, and R. C. Finkel (2001), Stochastic processes of soil production and transport: Erosion rates, topographic variation and cosmogenic nuclides in the Oregon Coast Range, *Earth Surf. Processes Landforms*, *26*(5), 531–552, doi:10.1002/esp.209.
Hunsinger, G. B., S. Mitra, J. A. Warrick, and C. R. Alexander (2008), Oceanic loading of wildfire-derived organic compounds from a small mountainous river, *J. Geophys. Res.*, *113*, G02007, doi:10.1029/2007JG000476.
Jackson, M., and J. J. Roering (2009), Post-fire geomorphic response in steep, forested landscapes: Oregon Coast Range, USA, *Quat. Sci. Rev.*, *28*(11–12), 1131–1146, doi:10.1016/j.quascirev.2008.05.003.
Jordan, P., and S. A. Covert (2009), Debris flows and floods following the 2003 wildfires in southern British Columbia, *Environ. Eng. Geosci.*, *15*(4), 217–234, doi:10.2113/gseegeosci.15.4.217.
Keeley, J. E. (1992), Demographic structure of California chaparral in the long-terms absence of fire, *J. Veg. Sci.*, *3*(1), 79–90, doi:10.2307/3236001.
Krammes, J. S. (1965), Seasonal debris movement from steep mountainside slopes in southern California, in *Proceedings of the Second Federal Interagency Sedimentation Conference*, pp. 85–89, U.S. Dept. of Agric., Washington, D. C.
Lavé, J., and D. Burbank (2004), Denudation processes and rates in the Transverse Ranges, southern California: Erosional response of a transitional landscape to external and anthropogenic forcing, *J. Geophys. Res.*, *109*, F01006, doi:10.1029/2003JF000023.
Los Angeles County Department of Public Works (L.A.C.D.P.W.) (1991), Hydrology Manual, reference guide, Los Angeles, Calif.
Los Angeles County Flood Control District (L.A.C.F.C.D.) (1959), Report on debris reduction studies for mountain watersheds of Los Angeles County, report, 164 pp., Los Angeles, Calif.
Mersereau, R. C., and C. T. Dyrness (1972), Accelerated mass wasting after logging and slash burning in western Oregon, *J. Soil Water Conserv.*, *27*, 112–114.
Moody, J. A., and D. A. Martin (2001), Initial hydrologic and geomorphic response following a wildfire in the Colorado Front Range, *Earth Surf. Processes Landforms*, *26*(10), 1049–1070, doi:10.1002/esp.253.
Reneau, S. L., D. Katzman, G. A. Kuyumjian, A. Lavine, and D. V. Malmon (2007), Sediment delivery after a wildfire, *Geology*, *35*(2), 151–154, doi:10.1130/G23288A.1.
Rice, R. M. (1974), The hydrology of chaparral watersheds, in *Symposium on Living with the Chaparral*, edited by M. Rosenthal, pp. 27–34, Sierra Club, San Francisco, Calif.
Rice, R. M. (1982), Sedimentaion in the Chaparral: How do you handle unusual events?, in *Sediment Budgets and Routing in Forested Drainage Basins*, edited by F. J. Swanson et al., *For. Serv. Gen. Tech. Rep. PNW-141*, pp. 39–49, U.S. For. Serv., Washington, D. C.
Roering, J. J., and M. Gerber (2005), Fire and the evolution of steep, soil-mantled landscapes, *Geology*, *33*(5), 349–352, doi:10.1130/G21260.1.
Rowe, P. B., C. M. Countryman, and H. C. Storey (1954), Hydrologic analysis used to determine effects of fire on peak discharge and erosion rates in southern California watersheds, report, 48 pp., U.S. Dep. of Agric., Water Resour. Cent. Arch., Univ. of Calif., Berkeley.
Santi, P. M., V. G. deWolfe, J. D. Higgins, S. H. Cannon, and J. E. Gartner (2008), Sources of debris flow material in burned areas, *Geomorphology*, *96*(3–4), 310–321, doi:10.1016/j.geomorph.2007.02.022.
Shakesby, R. A., and S. H. Doerr (2006), Wildfire as a hydrological and geomorphological agent, *Earth Sci. Rev.*, *74*(3–4), 269–307, doi:10.1016/j.earscirev.2005.10.006.
Spittler, T. E. (1995), Fire and debris flow potential of winter storms, in *Brushfires in California Wildlands: Ecology and Resource Management*, edited by J. E. Keeley and T. Scott, pp. 113–120, Int. Assoc. of Wildland Fire, Fairfield, Wash.
Spotila, J. A., M. A. House, A. E. Blythe, N. A. Niemi, and G. C. Bank (2002), Controls on the erosion and geomorphic evolution of the San Bernardino and San Gabriel Mountains, southern California, in *Contributions to Crustal Evolution of the Southwestern United States*, edited by A. Barth, *Spec. Pap. Geol. Soc. Am.*, *365*, 205–230, doi:10.1130/0-8137-2365-5.205.
Swanson, F. J. (1981), Fire and geomorphic processes, in *Fire Regime and Ecosystem Properties*, edited by H. A. Mooney et al., pp. 401–421, *For. Serv. Gen. Tech. Rep., WO-26*, U.S. For. Serv., Washington, D. C.
United States Department of Agriculture Forest Service (U.S.D.A.F.S.) (2009), Interagency fire history (perimeters), http://www.fs.fed.us/r5/rsl/clearinghouse/gis-download.shtml, Pac. Southwest Reg., Remote Sens. Lab., McClellan, Calif.
Wells, W. G. (1981), Some effects of brush fires on erosion processes in coastal southern California, in *Erosion and Sediment Transport in the Pacific Rim Steeplands*, edited by T. R. G. Davies and A. J. Pearce, *IAHS Publ.*, *132*, 305–342.
Wells, W. G. (1987), The effect of fire on the generation of debris flows in southern California, *Rev. Eng. Geol.*, *7*, 105–114.
Wohl, E. E., and P. P. Pearthree (1991), Debris flows as geomorphic agents in the Huachuca Mountains of southeastern Arizona, *Geomorphology*, *4*(3–4), 273–292, doi:10.1016/0169-555X(91)90010-8.
Zammit, C. A., and P. H. Zedler (1992), Size structure and seed production in even-aged populations of *Ceanothus greggii* in mixd chaparral, *J. Ecol.*, *81*, 499–511, doi:10.2307/2261528.

W. H. Amidon, M. P. Lamb, A. Limaye, J. S. Scheingross, and E. Swanson, Division of Geological and Planetary Sciences, California Institute of Technology, MC 170-25, 1200 E. California Blvd., Pasadena, CA 91125, USA. (mpl@gps.caltech.edu)